



Article

# Arbitrage Free Approximations to Candidate Volatility Surface Quotations

Dilip B. Madan <sup>1,\*</sup> and Wim Schoutens <sup>2,\*</sup>

<sup>1</sup> Robert H. Smith School of Business, University of Maryland, College Park, MD 20742, USA

<sup>2</sup> Department of Mathematics, KU Leuven, 3000 Leuven, Belgium

\* Correspondence: dbm@rhsmith.umd.edu (D.B.M.); wim.schoutens@kuleuven.be (W.S.)

Received: 19 February 2019; Accepted: 10 April 2019; Published: 21 April 2019



**Abstract:** It is argued that the growth in the breadth of option strikes traded after the financial crisis of 2008 poses difficulties for the use of Fourier inversion methodologies in volatility surface calibration. Continuous time Markov chain approximations are proposed as an alternative. They are shown to be adequate, competitive, and stable though slow for the moment. Further research can be devoted to speed enhancements. The Markov chain approximation is general and not constrained to processes with independent increments. Calibrations are illustrated for data on 2695 options across 28 maturities for *SPY* as at 8 February 2018.

**Keywords:** bilateral gamma; fast Fourier transform; sato process; matrix exponentials

**JEL Classification:** G10; G12; G13

## 1. Introduction

A variety of arbitrage free models for approximating quoted option prices have been available for some time. The quotations are typically in terms of (Black and Scholes 1973; Merton 1973) implied volatilities for the traded strikes and maturities. Consequently, the set of such quotations is now popularly referred to as the volatility surface. Some of the models are nonparametric with the Dupire (1994) local volatility model being a popular example. The local volatility model is specified in terms of a deterministic function  $\sigma(K, T)$  that expresses the local volatility for the stock if the stock were to be at level  $K$  at time  $T$ . Though the options quoted are many in number, ranging from a few hundred to thousands on a single underlying asset, the arbitrage free conditions thereon are considerably restrictive. As a result it is believed that the volatility surface has far fewer degrees of freedom than the number of traded options. Attempts are then made at parametric descriptions of implied volatilities directly, often with five to ten parameters for each of the traded maturities. For examples one may refer to Gatheral (2006). These parametric models can be open to arbitrage possibilities. On occasion conditions are developed on the parameters to ensure that the resulting model for the surface is arbitrage free (Fengler (2009), Gatheral and Jacquier (2014), and Guo et al. (2016)). Alternatively, numerous parametric models are written for the underlying stock price process resulting in option prices that are arbitrage free by construction. Well known examples include Merton (1976), Madan and Seneta (1990), Heston (1993), Eberlein and Keller (1995), Barndorff-Nielsen (1998), Madan et al. (1998), Kou (2002), Eberlein and Prause (2002), Carr et al. (2002), Niccolato and Vernados (2003), Carr and Wu (2003), Carr et al. (2007) and Carr and Nadtochiy (2017) to mention a few.

It is known that the arbitrage free property is equivalent to the existence of a one dimensional Markov martingale model for the suitably discounted asset price with option prices then given as expectations of suitably discounted option payoffs under the specified martingale probability

(Kellerer 1972; Carr and Madan 2005; Davis and Hobson 2007). Among the martingale models there are numerous examples of higher dimensional stochastic evolutions, as evidenced by the Heston (1993), Carr et al. (2003) and Niccolato and Vernados (2003) stochastic volatility models, with the martingale property holding for just the discounted asset price and not for the auxiliary variables like the volatility. Since these models produce initial option prices free of static arbitrage there therefore then also exists a one dimensional Markov martingale consistent with the option prices being discounted expectations under this one dimensional Markov process that is often not exhibited. An example of such a Markov martingale could be the local volatility model derived from the stochastic volatility option prices at the initial time. The focus of this paper however, will be on parsimonious parametric one dimensional Markov martingale models for the suitably discounted asset price.

Many of the examples of such models in the literature are given by processes of independent increments that may or may not be time homogeneous. The time homogeneous processes are examples of Lévy processes that do not fit well across maturities (Konikov and Madan 2002). Lévy processes provably have the skewness and excess kurtosis of the return distribution decreasing like the reciprocal of the square root of the horizon and the horizon respectively. Observed market implied distributions do not possess such sharp rates of decline in these higher moments. Additive or processes with a specific time inhomogeneity based on scaling self decomposable laws at unit time were introduced in Carr et al. (2007). They were termed Sato processes following their development by Sato (1991). It was shown that they provide an adequate fit to the option prices across both the strike and maturity domains with a few (or four to five) parameters.

Most of these models, via independence across time, formulate analytical characteristic functions for the return density at arbitrary horizons. The technology of fast Fourier transforms introduced in Carr and Madan (1999) then yields call option prices directly on a Fourier inversion of analytical transforms for the suitably exponentially dampened call option prices. The method works well for relatively near-the-money option strikes with log forward strike ratios within 20 to 40 percent in absolute value. However, post the financial crisis of 2008 the market depth in downside strikes has expanded considerably as documented later in this paper. For extremal strikes in the two tails we observe that model prices obtained by Fourier inversion have difficulties in calibrating to their quoted counterparts. After numerous attempts with a variety approaches at calibrations using Fourier inversion, not reported here, we concluded that for the wide range of option strikes now being actively quoted one may need to change the pricing technology away from Fourier inversion of characteristic functions. The reliance on independence built into some characteristic functions is also a further restriction that it may be advantageous to avoid.

Before moving on in an alternate direction it is worth noting that there have been extensions of Fourier methods with respect to dealing with deep out of the money options. One such approach is the use of saddle point approximations developed in Rogers and Zane (1999), Xiong et al. (2005), and Carr and Madan (2009) for example. However the approximations are particular to each strike and maturity and it is not clear what underlying process will tie all the approximations together in a single process approximation for all strikes and maturities. Yet another approach is to invert for the density adopted in Fang and Oosterlee (2008) and Kirkby (2015) and then integrate the payoff against the density. The option prices themselves are smoother objects than distribution functions that are smoother than densities and we anticipate that inversions for second derivatives in tails should generally be more problematic than the inversion for the option price. In any case our interest is also to enhance the use of models not amenable to the presence of analytical characteristic functions.

We therefore turn our attention to calibrating one dimensional Markov processes that permit the transition densities to be both time inhomogeneous and depend nonlinearly on the level of the underlying asset price. A possible solution is to employ finite state continuous time Markov chain approximations to describe state transition rate matrices as introduced in Mijatović and Pistorius (2011). The matrix exponentials of these matrices deliver probability elements that on multiplication across time steps permit time inhomogeneity in the formation of risk neutral density approximations at arbitrary

horizons. These probability elements may be used to compute the model option prices. The state spaces used may employ the use of non-uniform grids, concentrated near the forward. The objective here is to report on the use of such an approach for the volatility surface on *SPY* as at 8 February 2018 as a test case. This option surface had 2695 option prices across 28 maturities between a few days to two years.

The outline for the rest of the paper is as follows. Section 2 documents the growth in the traded options, their moneyness spreads, and the number of maturities being traded across time. The need to cope with this expansion using one dimensional Markov models is then set by the requirements induced by the absence of static arbitrage. These conditions are briefly reviewed in Section 3. Section 4 reports on the difficulties faced by Fourier inversion methodologies on our test data set. Section 5 presents arguments for the selection of parametric models describing the local motion of the underlying asset price. Section 6 develops the mechanics for finite state continuous time Markov chain approximation methodologies. Results based on spatial homogeneity and time inhomogeneity for our test case data set are presented in Section 7. Section 8 reports results for stylized models permitting spatial inhomogeneity coupled with time homogeneity. Section 9 reports results for both time and spatial inhomogeneity for our test case. Section 10 concludes.

## 2. Option Trading Over Time

The number of options traded, their moneyness and the number of maturities quoted have been developing over time. Back in the late 1990s, when Fourier transform technology was developed, the concern was over a few hundred options across some ten maturities for the index options and a smaller set for single names. The range of moneyness measured as the log strike to forward ratio was within typically plus or minus 30%. The Fourier methodology served this purpose well for the decade 1998–2008. The year 2008 was hit by a financial crisis demonstrating substantial downward moves in asset prices occurring over a short period that was well within existing option maturities. The result has been a growth in the number of options being traded, their moneyness spread and the number of maturities being traded.

Here we first present graphs for the number of option quotes, their moneyness levels and the number of maturities quoted below the maturity of two and a half years over the period 2001 to 2018 for the S&P 500 Index (*SPX*) as the underlying asset. Also presented are graphs for options on *SPY* the exchange traded fund tracking the *SPX* over the period 2013–2018. Figure 1 presents kernel smoothed data on these magnitudes.

The number of options traded has grown to a few thousand while the number of maturities has more than doubled to over 20. The moneyness on the down side has moved substantially. The shifts have occurred since the crisis of 2008. Since 2014 we have weekly options trading and initially the expiries were on Friday but now also include Mondays and Wednesdays. The time to maturity can then be as low as a few days with a substantial strike range. At some intermediate and longer maturities we also have a large number of strikes trading that are quite far from the forward and pose particular problems for Fourier inversion technology. The data sets call for new pricing technologies and after reviewing the associated no arbitrage requirements we go on to develop one such technology.

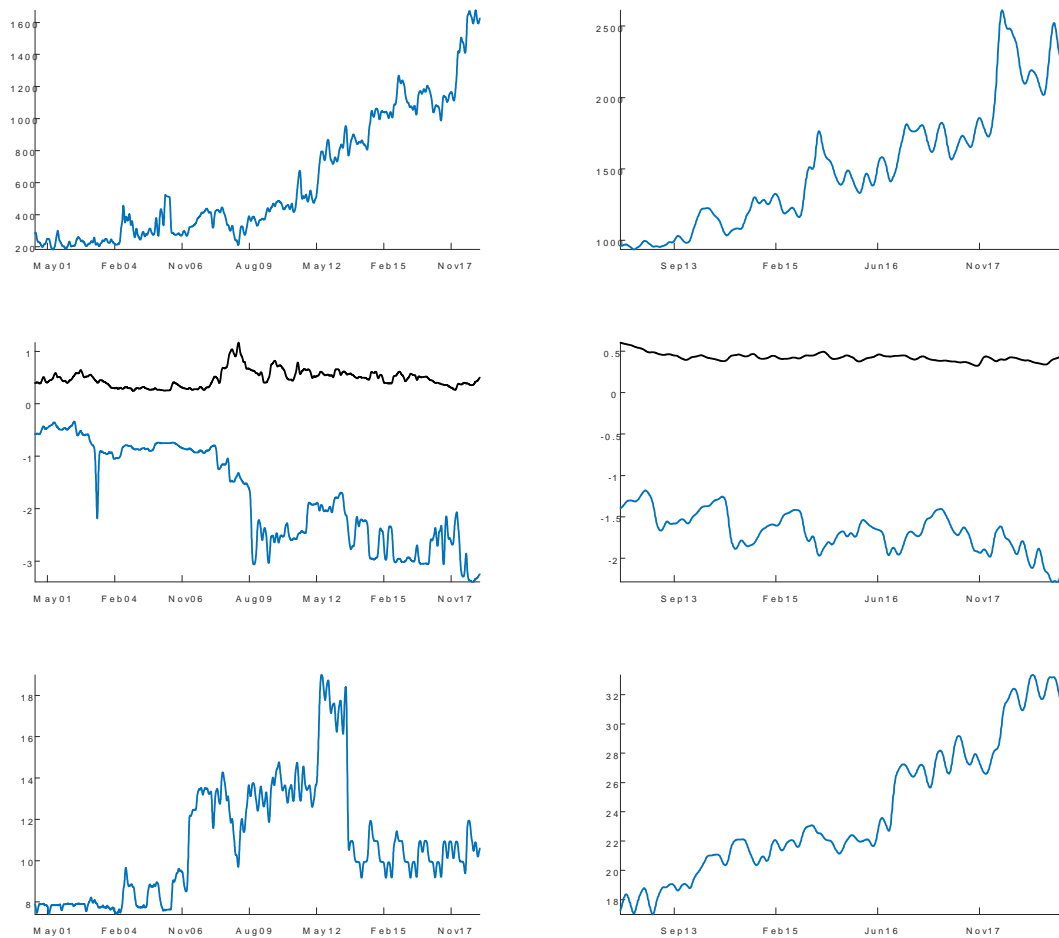


**Figure 1.** The left panel presents results for the SPX while the right panel presents comparable results for SPY. The time period for the SPX is 2001–2018 while for SPY it is 2013–2018. The top row is for the number of options traded. The middle row show the highest and lowest levels of moneyness measured by the log strike to forward ratio. The bottom row presents the number of maturities traded.

### 3. No Arbitrage Considerations

Suppose we have out of the money European option prices  $w(K, T)$  for strike  $K$  and maturity  $T$ , on an underlying asset with current spot price  $S_0$  and forward price  $F_T$  for maturity  $T$ . For  $K \leq F_T$  the price is that for a put options while for  $K \geq F_T$  the price is that of a call option. The respective payoffs are  $(K - S_T)^+$  and  $(S_T - K)^+$  where  $S_T$  denotes the unobserved price of the asset at time  $T$ . Let  $B(T)$  denote the current discount curve or the price of a risk free dollar promised at time  $T$ . A static arbitrage is a trade initiated today with all positions being held to the longest maturity accessed at zero initial cost that unwinds at a nonnegative, nonzero, final (at longest maturity held) outcome. In the absence of static arbitrage nonnegative, nonzero final outcomes must have a positive current cost. Furthermore, under the law of one price the value of a linear combination of positions must be the value of the same linear combination of their payoffs. As a consequence (Ross 1978) for each fixed  $T$  there exists a state pricing kernel  $h(S, T)$  such that for a portfolio of positions delivering  $c(S)$  its value  $V(c)$  is

$$V(c) = \int_0^\infty c(S)h(S, T)dS.$$

In particular

$$B(T) = \int_0^\infty h(S, T)dS.$$

From the absence of static arbitrage the value of nonnegative, nonzero  $c$ 's are positive and hence  $h$  is nonnegative. Defining a probability density  $q(S, T)$  by

$$q(S, T) = \frac{h(S, T)}{B(T)}$$

we observe that

$$V(c) = B(T) \int_0^\infty c(S) q(S, T) dS$$

or that valuations are given by discounted expected values taken with respect to the market implied densities  $q(S, T)$ . In particular

$$\frac{w(K, T)}{B(T)} = \int_0^\infty \left[ (S - K)^+ + \mathbf{1}_{K < F_T} (K - S) \right] q(S, T) dS.$$

Differentiation with respect to  $K$  (Breedon and Litzenberger 1978) yields that the absolute value of the derivative is a tail probability under the density  $q$

$$\frac{|w_K(K, T)|}{B(T)} = Q([S \leq K] \mathbf{1}_{K < F_T} + [S > K] \mathbf{1}_{K > F_T}),$$

where  $Q(A) = \int_A q(S, T) dS$ . Thus the static arbitrage free option prices contain valuable information on the implied pricing densities.

Since the forward contract delivering  $S_T - F_T$  at time  $T$  has a zero initial cost it follows that

$$F_T = \int_0^\infty S q(S, T) dS.$$

It follows that  $s_T = S_T / F_T$  has densities  $\tilde{q}(s, T)$  that all have a unit expectation. Explicitly we have that

$$\tilde{q}(s, T) = q(F_T s, T) F_T.$$

It is shown in Appendix A that these densities are increasing in the convex order. As a consequence there exists a one dimensional Markov martingale  $M(t)$  (Kellerer 1972, Carr and Madan 2005, Davis and Hobson 2007) starting at unity with probability law  $Q^M$  such that for all  $T$

$$\int_0^\infty (s - k)^+ \tilde{q}(s, T) ds = E^{Q^M} [(M(T) - k)^+].$$

Numerous papers focus attention on conditions to be placed on implied volatilities consistent with positive values for butterfly and calendar spread arbitrages and thereby the absence of arbitrage with no explicit construction of the implied one dimensional Markov martingale. The focus here will be on such explicit constructions.

The supposition of this section so far of assuming that one has access to option prices free of static arbitrage is generally false. What one may have is access to best bid and offer prices that are not necessarily simultaneously updated but with some level of synchronicity for end of day prices. Mid quotes for volatilities may be constructed using some weighting structures or least squares approximations delivered by models to such. It is not at all clear that the resulting prices are arbitrage free. Nonetheless, for various marking and valuation purposes there is an interest in constructing arbitrage free approximations to such potentially arbitrageable mid quote constructions. Hence the fitting of option quotes exactly, using arbitrage free frameworks, is not even to be attempted. The observed prices are to be treated as perhaps close to some arbitrage free collection and only approximations to these candidate quotes are being sought.

#### 4. Fourier Transform Issues

Fourier transform-based pricing especially when it is conducted using the fast Fourier transform is very efficient and fast. The construction exploits the fact that the large step characteristic function is based on multiplying the characteristic functions relevant for various subintervals. In this regard it is well suited to regime switching models as developed for example in [Elliott and Osakwe \(2006\)](#). More generally they are applicable when infinitesimal generators are linear in state variables ([Duffie et al. 2000, 2003](#)). However, there is a deficiency in the approach that arises for extreme strikes far out in the tails where the calculations can be unstable. The instability arises as trigonometric approximations get oscillatory with unreliable sums as one gets further out in the tails.

We recognize that the Fourier transform approach has significant advantages, not least among which is its speed. It is more than adequate for numerous applications and the objective is not to diminish these features that we continue to employ in a variety of contexts. The intention is to develop and advance the Markov chain approximation as an alternate that has its own advantages and possible applications. The particular Fourier pricing approach being reported on here is that of [Carr and Madan \(1999\)](#) with  $2^{14}$  points delivering prices at strikes determined by the strike spacing. The prices for actual traded strikes are interpolated from these values. The method has been widely implemented for some twenty years now and we were motivated to consider the Markov chain method on observing problems in this traditional method in the extreme tail strikes now being traded. Additionally, the Markov chain method has its own advantages when infinitesimal generators are no longer linear in state variables as is the case for affine processes by construction.

To highlight this issue we take the logarithm of the stock to be driven by a bilateral gamma Lévy process introduced in detail later in the paper and construct the option prices in two ways for a stylized parameter set. The first way is to employ an 800 point finite state continuous time Markov chain approximation building transition rate matrices whose matrix exponential raised to power of the time horizon delivers the probability element that may be used to evaluate option prices. The second uses the classical Fourier inversion methodology. For the bilateral gamma parameter set  $b_p = 0.0906$ ,  $c_p = 0.5183$ ,  $b_n = 0.3501$ ,  $c_n = 0.4805$  with a maturity of 0.04 and strikes ranging from 30 to 130 for a spot of 100 and zero rates and dividend yields Figure 2 presents both calculations.

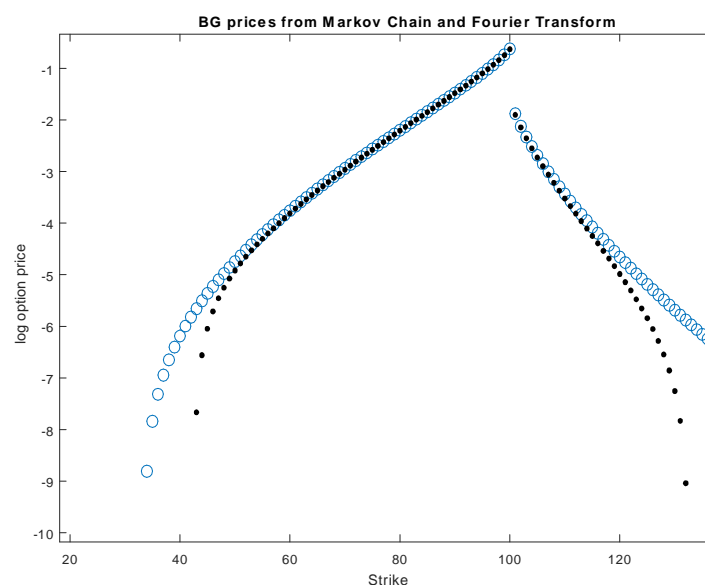


**Figure 2.** Out of the money log option prices as functions of strike at the maturity 0.04 for bilateral gamma parameters 0.0906, 0.5183, 0.3501, 0.4805 for  $b_p$ ,  $c_p$ ,  $b_n$ , and  $c_n$  respectively. The Markov chain approach is shown in circles while the Fourier transform approach is presented by dots.

On actual data we estimated the bilateral gamma model separately for each of 28 maturities for SPY options as at 20180208 by the Fourier transform methodology and present a sample of model log prices as functions of strike along with log quoted price at a handful of nine sample maturities in Figure 3. The regions where put prices decline and call prices increase are when model prices have gone negative. We observe an inability in model performance especially at the shorter maturities.

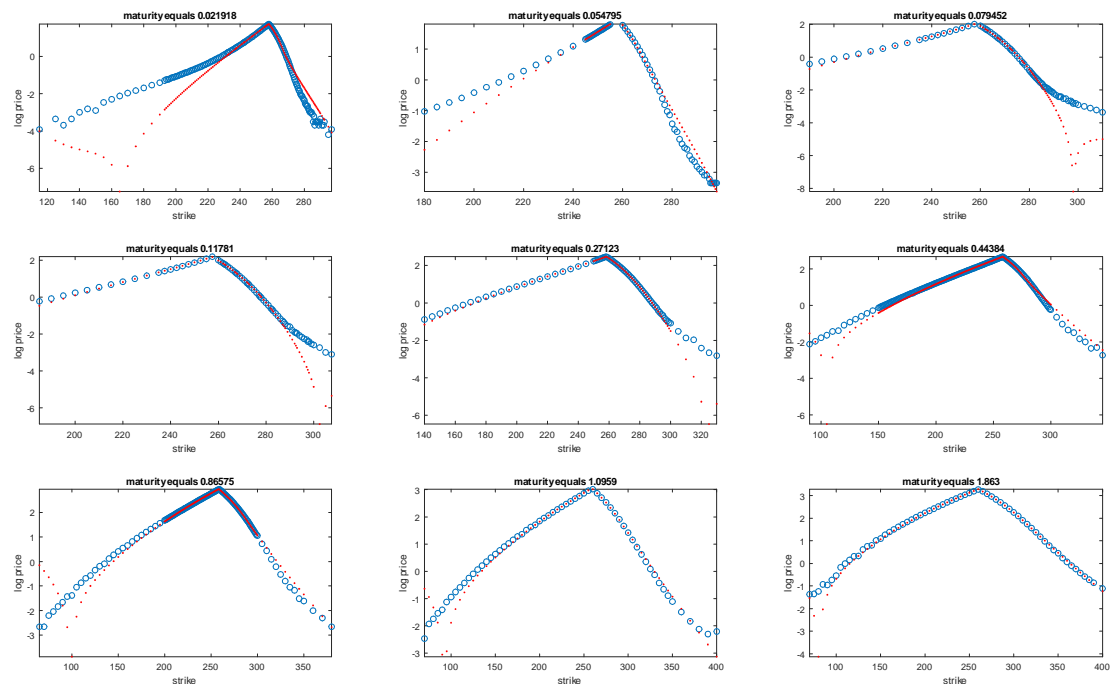


**Figure 3.** Fit of bilateral gamma to SPY options separately at several maturities. Circles show quoted log out of the money option prices, while dots reflect model log prices.

For three maturities where the results were not good the graphs are presented in Figure 4.

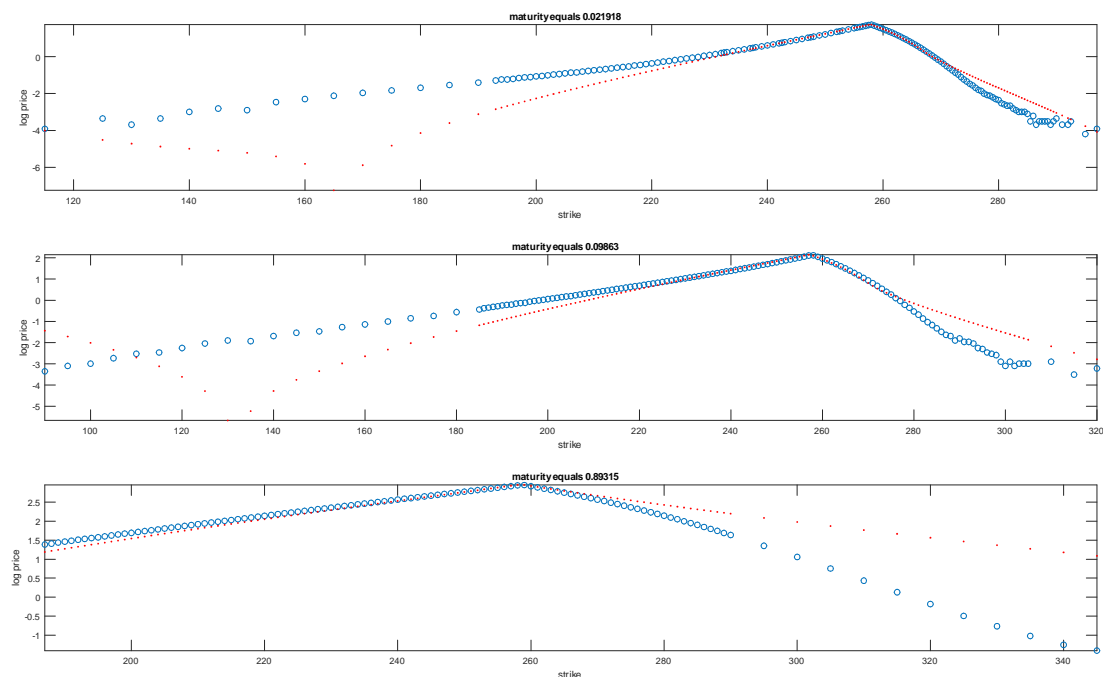


**Figure 4.** log out of the money option price fits at three difficult maturities.



One observes that here the strike range is very wide indeed and this has impacted the ability of the optimizer to cope with the required calibration when constrained to Fourier inversion. Given the ability of Markov chain approximations to be more stable over a wider range and their ability to cope with the absence of independence in evolution we turn our attention to developing this methodology as an alternative particularly relevant to current market conditions where strike ranges of interest have grown considerably.

Table 1 presents a sample of fitted and quoted out-of-the-money put option prices for *SPY* as at 27 December 2017 for the maturity of 23 days.

**Table 1.** Sample of Fitted OTM Put Option Prices for *SPY* on 27 December 2017 for a maturity of 23 days with the spot price at 267.28.

Strike	Market Price	Fitted Price
221	0.0550	0.0232
225	0.0650	0.0344
230	0.0950	0.0543

## 5. Modeling Transition Rates

For a one dimensional Markov process for the asset price  $S(t)$  or more exactly its logarithm  $X(t)$  one has to specify the law of motion as a function of the level of the process  $X$  and the current time  $t$ . A classical example is the risk neutral Dupire local volatility model where the local motion is a Brownian motion with some volatility  $\sigma(X, t)$  and drift equal to the interest rate  $r$  for the asset price and  $r - \sigma(X, t)^2/2$  for the logarithm. This is a very restrictive single parameter local motion. It is a maximal entropy law conditional on the drift and variance level. The literature has however questioned the relevance of the use of a normal distribution with respect to calendar time. Clark (1973) and Ané and Geman (2002) have argued for the use of the normal distribution with respect to a random time change related to economic activity. Specific models incorporating such random time changes include the variance gamma model of Madan and Seneta (1990) and Madan et al. (1998) among others. Some other examples are presented in Barndorff-Nielsen (1998), and Eberlein and Keller (1995). More recently, Madan et al. (2018) argue that for a maximal entropy time change the time change should follow a gamma distribution and this delivers the variance gamma model of Madan and Seneta (1990). It was already observed in Madan and Seneta (1990) that the variance gamma model is a difference of two independent gamma processes each separately modeling the upward and downward motion of markets. Differentiating the drift on the two sides delivers the three parameter variance gamma model of Madan et al. (1998) that may also be cast as Brownian motion with drift time changed by a gamma process with unit and a positive variance rate. When written as the difference of two gamma processes the two processes have the same speed or variance rates but different scaling coefficients. More recently Madan and Wang (2017), Madan et al. (2017) have argued for differentiating the speeds for the upward and downward processes on noting that data support smaller and more frequent up moves as compared to the downward moves. These observations are consistent with the remark that markets take the escalator up and the elevator down. This kind of asymmetry is also reflected in the widening downside moneyness reported earlier relative to the stable up side moneyness levels. The difference of two gamma processes with differing scale and speed on both sides is referred to as the bilateral gamma model as first introduced in Küchler and Tappe (2008). Madan et al. (2018) also note that maximal entropy considerations for upward and downward motions suggest gamma process models for the two sides. These considerations suggest the use of a four parameter bilateral gamma model for the local motion of the logarithm of the asset price. There is uncertainty in both directions and this uncertainty has separate directional drifts and volatility rates suggestive of a minimal four parameter model for the local motion. A classical exponential correction is employed to lock in the right forward price, thereby formulating martingale models for the asset price relative to the forward as is required by the no arbitrage conditions.



The standard gamma process  $\gamma(t)$  has time  $t$  density  $p_\gamma(x, t)$  given by

$$p_\gamma(x, t) = \frac{x^{t-1}e^{-x}}{\Gamma(t)}, \quad x > 0.$$

The characteristic function is

$$\phi_\gamma(u) = \left( \frac{1}{1 - iu} \right)^t.$$

The process is an infinitely divisible increasing pure jump process with Lévy density

$$k_\gamma(x) = \frac{e^{-x}}{x}, \quad x > 0.$$

The general gamma process has scale and speed coefficients  $b, c > 0$  with the process being

$$g(t) = b\gamma(ct)$$

with density  $p_g(x, t)$  given by

$$p_g(x, t) = \frac{x^{ct-1}e^{-x/b}}{b^{ct}\Gamma(ct)}, \quad x > 0.$$

The characteristic function is

$$\phi_g(u) = \left( \frac{1}{1 - iub} \right)^{ct}$$

and Lévy density

$$k_g(x) = c \frac{e^{-x/b}}{x}, \quad x > 0.$$

The bilateral gamma process is the difference of two independent gamma processes with parameters for the positive and negative components of  $b_p, c_p$  and  $b_n, c_n$  respectively with

$$X(t) = b_p\gamma_p(c_pt) - b_n\gamma_n(c_nt)$$

where  $\gamma_p, \gamma_n$  are two independent gamma processes. The characteristic function for  $X$  is

$$\phi_X(u) = \left( \frac{1}{1 - iub_p} \right)^{c_pt} \left( \frac{1}{1 + iub_n} \right)^{c_nt}.$$

The Lévy density is

$$k_X(x) = c_p \frac{e^{-x/b_p}}{x} \mathbf{1}_{x>0} + c_n \frac{e^{-|x|/b_n}}{|x|} \mathbf{1}_{x<0}.$$

We take the local motion to be bilateral gamma where all the four parameters may depend nonlinearly on  $X, t$  using deterministic functions  $B_p(X, t)$ ,  $C_p(X, t)$ ,  $B_n(X, t)$ , and  $C_n(X, t)$ . The bilateral gamma process has a complicated probability density identified in [Kühler and Tappe \(2008\)](#). However, in building transition rates the Lévy measures suffice and they are analytical and fairly simple.

## 6. Continuous Time Markov Chain Approximations

The first step in building continuous time Markov chain approximations to Markov processes is to define the state space. Here we follow [Mijatović and Pistorius \(2011\)](#) to employ a non-uniform grid for the state space. The total number of points  $M$  is taken to even, while  $a, b$  are the lowest and highest

values for the logarithm of the spot price. The current value is  $s$ . There are two density parameters  $g_1$ , and  $g_2$  and on setting  $c_1 = \operatorname{arcsinh}((a-s)/g_1)$  and  $c_2 = \operatorname{arcsinh}((b-s)/g_2)$  the grid is defined by

$$\begin{aligned}x_k &= s + g_1 \sinh \left( c_1 \left( 1 - \frac{k-1}{M/2-1} \right) \right), \quad k = 1, 2, \dots, M/2 \\x_{k+M/2} &= s + g_2 \sinh \left( \frac{c_2 2k}{M} \right), \quad k = 1, 2, \dots, M/2.\end{aligned}$$

We employed a low volatility of 5% and set  $g_1 = g_2 = 0.0025$ . Note that  $x_1 = a$ ,  $x_{M/2} = s$  and  $x_M = b$ .

The next step is the construction of the transition rate matrix  $A_{ij}$  from state  $i$  to state  $j$  at time  $t$ . For all rows  $A_{ii} = -\sum_{j \neq i} A_{ij}$ . The current state is  $x_i$  and we seek the transition rates to states  $j \neq i$ . The first and last rows of  $A$  are identically zero to kill the process at these boundaries. For rows 3 to  $M-2$  we proceed as follows. One first looks up the deterministic functions however specified to obtain  $b_p = B_p(x_i, t)$ ,  $c_p = C_p(x_i, t)$ ,  $b_n = B_n(x_i, t)$ , and  $c_n = C_n(x_i, t)$  and set  $\theta = (b_p, c_p, b_n, c_n)$ .

For  $j > i+1$ , and  $j < i-1$ , thereby ignoring for now the immediately upper and lower diagonals, one defines the jump size distance

$$\begin{aligned}z_{j,u} &= \frac{x_{j+1} + x_j}{2} - x_i \\z_{j,d} &= \frac{x_j + x_{j-1}}{2} - x_i\end{aligned}$$

The transition rates are defined in terms of tail measure functions

$$K(x; \theta) = \int_{-\infty}^x k_X(y) dy \mathbf{1}_{x < 0} + \int_x^{\infty} k_X(y) dy \mathbf{1}_{x > 0}.$$

Specifically

$$A_{ij} = \left( K(z_{j,d}, \theta) - K(z_{j,u}, \theta) \right) \mathbf{1}_{x_j > x_i} + \left( K(z_{j,u}, \theta) - K(z_{j,d}, \theta) \right) \mathbf{1}_{x_j < x_i}.$$

For the upper and lower diagonal we need to determine the two value  $A_{i,i-1} = p_1$  and  $A_{i,i+1} = p_2$ . For this purpose if the local quadratic variation is high enough or above a threshold, we employ a diffusion approximation. Otherwise we just organize getting drift correct for the move in the stock price.

Let  $u = x_{i+1}$  and  $d = x_{i-1}$ . The total quadratic variation is  $v_A = b_p^2 c_p + b_n^2 c_n$  while the local quadratic variation is the integral of  $x^2$  against the Lévy measure in the interval  $c_1, c_2$  where  $c_1 = (x_{i-2} + x_{i-1})/2$  and  $c_2 = (x_{i+1} + x_{i+2})/2$  that we denote by  $v_L$ . We employed the diffusion approximation if  $v_L > 0.01 v_A$ . For this approximation the vector  $p = (p_1, p_2)'$  satisfies

$$Gp = b$$

where

$$G = \begin{pmatrix} e^{d-x_i} & e^{u-x_i} \\ (d-x_i)^2 & (u-x_i)^2 \end{pmatrix}$$

and defining  $\beta = \sum_{j, |j-i| > 1} A_{ij}(e^{x_j} - e^{x_i})$  set

$$b = \begin{pmatrix} (r-q)e^{x_i} - \beta \\ v_L \end{pmatrix}.$$

When  $v_L$  is below one percent of the aggregate quadratic variation  $v_A$  we just monitor the drift and define

$$\zeta = (r-q)e^{x_i} - \beta.$$

If  $\zeta > 0$  we set  $p_1 = 0$  and set  $p_2 = \zeta / (e^u - e^{x_i})$  while for  $\zeta < 0$  we set  $p_2 = 0$  and  $p_1 = \zeta / (e^d - e^{x_i})$ .

For the second row we take the third from the second element onwards followed by a trailing zero with diagonal reset as the negative of the off diagonal. Similarly for last but one we take the first  $N - 1$  elements of the last but two starting with an initial zero and reset the diagonal. This completes the definition of a transition rate matrix at a particular  $t$ .

Transition rate matrices  $A^j$  are defined at a finite set of time points  $t_j$  for  $j = 1, \dots, n$  using the space dependence for this maturity that applies for all times  $t < t_j$  and greater than  $t_{j-1}$ . To access the probability element at an arbitrary time  $t$  let  $k$  be the largest  $j$  below  $t$ . The probability element at time  $t$  is given by the central row of

$$P(t) = \left( \prod_{j \leq k} \exp \left( A^j (t_j - t_{j-1}) \right) \right) \exp \left( A^{k+1} (t - t_k) \right).$$

This probability element is then used to price options at time  $t$  by discounting expected payouts using the probability element.

Though attention is restricted here to one dimensional Markov process approximations the general method of Markov chain approximations has been extended to multifactor models in Cui et al. (2017) and Kirkby et al. (2017). Stochastic local volatility extensions may be found in Cui et al. (2018) along with a rigorous error analysis in Li and Zhang (2017). The time dependence is however accommodated in a piecewise fashion as opposed to employing smooth functions for the time dependence as appear in local volatility models of Dupire (1994) and Carr et al. (2003).

## 7. Bilateral Gamma Extensions

As already noted the data set for the results reported in this paper are options on *SPY* as at 8 February 2018 comprising 2695 options over 28 maturities. Two sets of results are presented, one for the Fourier transform approach applied to the Sato process based on the bilateral gamma model at unit time across all 28 maturities. The second employs bilateral gamma evolution in each of seven time intervals using a continuous time Markov chain approximation with no space inhomogeneity as the parameters are kept invariant to the current stock price. There is only a time dependence in the transition rate matrices  $A^j$  for  $j = 1, \dots, 7$ . These results are reported in separate subsections.

### 7.1. Fourier Transform Applied to the Sato Process Based on The Bilateral Gamma

The Sato process based on the variance gamma model was introduced in Carr et al. (2007) on recognizing that Lévy processes were structurally incapable of fitting option prices across maturities. It was observed in Konikov and Madan (2002) that all Lévy processes by virtue of the linearity of the characteristic exponent in time, had skewness and excess kurtosis of term return distributions that fell like the reciprocal of the square of the term or the term respectively. However, these entities may be estimated model free from option prices using the results of Breeden and Litzenberger (1978) to determine that they may be constant or slightly increasing or decreasing with the term, but definitely not decreasing at rates embedded in Lévy processes. These observations led Carr et al. (2007) to consider time scaling and make links to the works of Sato (1991). Sato showed that for a subclass of infinitely divisible laws and hence laws of Lévy processes at unit time termed self-decomposable laws one may also associate with them an additive process that reproduces as its marginal distributions the distribution at unit time scaled by a function of time. Furthermore if one invokes the hypothesis of self similarity the scaling function reduces to a power function of the time to maturity. Carr et al. (2007) observed that the variance gamma model had a unit time distribution that was self decomposable and hence the additive process identified by Sato was available as a candidate process possibly consistent with return distributions embedded in option prices across maturities. Empirical work reported in their paper confirmed the adequacy of such processes now called Sato processes as adequate models for option data across strike and maturity. They reported on the performance of a variety of self

decomposable laws with the variance gamma being among the simplest and empirically adequate ones. One easily observes that the bilateral gamma extension of the variance gamma is also self decomposable and hence there is a Sato process associated with the bilateral gamma model at unit time.

It is also worth noting that self decomposable laws were characterized by Lévy (1937) and Khintchine (1938) as limit laws much like the Gaussian law itself on allowing more general scaling functions than the square root of the number of independent of shocks being averaged in taking the limit. Given the large number of potential news events and shocks being responded to in markets over a short period like day or so, it seems reasonable to restrict modeling attention to such limit laws at unit time. We therefore proceed here with the Sato process associated with the bilateral gamma model at unit time. Let  $X$  be a bilateral gamma law at unit time with parameters  $b_p$ ,  $c_p$ ,  $b_n$ , and  $c_n$ . The marginal laws at other maturities  $t$  for the Sato process are given by

$$X(t) \stackrel{(d)}{=} t^\gamma X$$

for a scaling coefficient  $\gamma$ . The characteristic function for  $X(t)$  is then derived as

$$\begin{aligned}\phi_{X(t)}(u) &= E[\exp(iuX(t))] \\ &= \left(\frac{1}{1 - iut^\gamma b_p}\right)^{c_p} \left(\frac{1}{1 + iub_n t^\gamma}\right)^{c_n}.\end{aligned}$$

Hence the Sato process model termed *bgssd*, after scaled self decomposable associated with the bilateral gamma, is five parameter model including the scaling parameter  $\gamma$  along with the four bilateral gamma parameters.

This model was fit to all 2695 options on *SPY* as at 8 February 2018 using the Fourier inversion methods of Carr and Madan (1999). The result of the fit is presented in Figure 5 that also reports the parameter values and fit statistics. An average percentage error of near nine percent is a bit too high to consider the model as an acceptable one for many applications. One may observe some of the poorer fits in the tails on a log price plot, a feature characteristic of Fourier methods for strikes this far out.

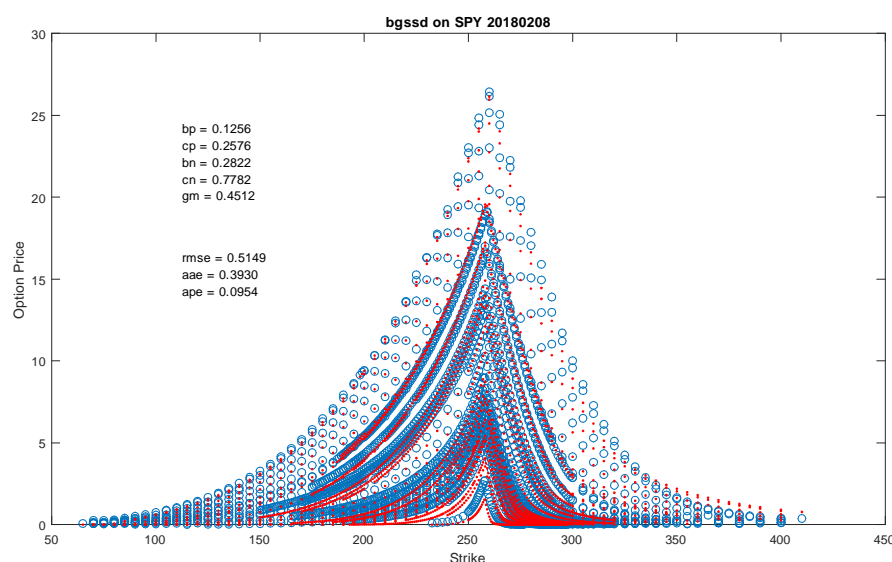


**Figure 5.** Fit of *bgssd* to *SPY* options as at 8 February 2018. Shown by circles are the out of the money market prices for the 2695 across 28 maturities. The dots represent the calibrated model prices. Also presented are parameter values and fit statistics.

### 7.2. Forward Bilateral Gamma via Markov Chain Approximation

The forward bilateral gamma construction supposes that the bilateral gamma parameters for the local motion of the logarithm of the asset price depend just on calendar time and are independent of the level of the asset price. Here we also take the dependence on time to be piecewise constant with a pre-specified set of time points at which the parameters change. For our test case of the SPY as at 8 February 2018 we have all maturities below 2 years. The pre-specified time points for parameter shifts were set at a week, a month, a quarter, a half year, a year, a year and a half and two years. The parameters relevant for an arbitrary time point  $t$  are those for the smallest pre-specified point above  $t$ . The total number of pre-specified time points is seven and with four bilateral gamma parameters to be estimated at each of these time points we have  $28 = 7 \times 4$  parameters in the forward bilateral gamma model. The parameters are used to build seven transition rate matrices  $A^j, j = 1, \dots, 7$  for the time points  $t_1, t_2, \dots, t_7$ . The Markov chain approximation then delivers the probability elements for arbitrary  $t$  that is used to evaluate expected payouts discounted to time zero for the option prices.

Figure 6 presents a graph of the fit along with fit statistics. The calibrated parameter values are presented in a matrix displaying seven rows for the four bilateral gamma at each pre-specified time point.

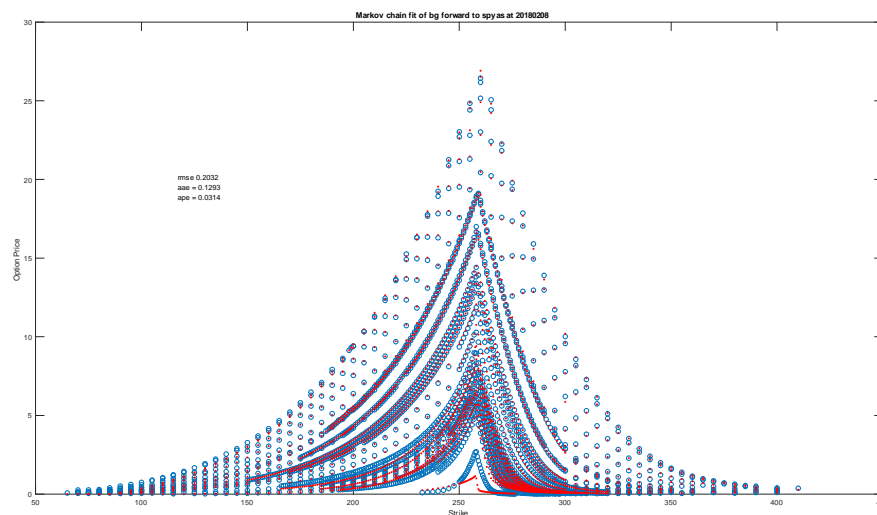


**Figure 6.** Fit of bgforward to SPY as at 8 February 2018 using Markov chain approximations.

The calibrated parameter matrix was as follows Table 2. The four columns present the values for  $b_p$ ,  $c_p$ ,  $b_n$ , and  $c_n$ .

**Table 2.** Forward Parameter Values.

Time Point	$b_p$	$c_p$	$b_n$	$c_n$
0	0.0549	6.9100	0.1347	14.9688
1	0.0161	5.5545	0.0611	12.0395
2	0.0386	1.0721	0.5095	0.4826
3	0.0696	0.9860	0.3482	0.4805
4	0.1621	0.0448	0.3064	0.5156
5	0.1039	0.3846	0.6833	0.1778
6	0.0435	0.3566	0.2448	0.7106

## 8. Stylized Bilateral Gamma Spatially Inhomogeneous and Temporally Homogeneous Model Results

Before attempting a calibration of a spatially inhomogeneous model on our test data set we first report on an investigation of a calibration on a stylized data set where the exact dependence of parameters on the underlying asset price is known by construction. The dependence of parameters on the logarithm of underlying asset price was modeled using logistic functions of the form

$$h(x) = \alpha_0 + (\alpha_1 - \alpha_0) \frac{1}{1 + \exp(-\theta x)}$$

whereby  $\alpha_0$  is the left limit for the parameter value while  $\alpha_1$  is the right limit and  $\theta$  controls the speed of transition. The stylized data was generated using  $\theta = 20$  with the left and right limits for the four parameters as presented in Table 3.

**Table 3.** Left and Right Limits for bilateral gamma parameters as functions of moneyness.

Parameter	Left Limit	Right Limit
$b_p$	0.07	0.0632
$c_p$	0.7886	2.4291
$b_n$	0.1854	0.2802
$c_n$	1.8992	1.4439

This parametric dependence was used to generate stylized true option values at four maturities of 3, 6, 9, and 12 months for 101 strikes ranging from 50 to 150 in steps of a dollar with the spot at 100 and zero rates and dividends. A graph of these prices against their strikes for all four maturities is presented when the calibration fit is later displayed.

For the space dependence to be calibrated we do not suppose any knowledge of the functional form of this dependence. Hence we cannot estimate the parameters of the logistic function. Instead we fix a grid of seven points for the log price relative to the forward. These values were taken at  $-0.5$ ,  $-0.2$ ,  $-0.1$ ,  $-0.05$ ,  $0.05$ ,  $0.15$ , and  $0.3$ . For a starting value for the parameters we take the value of the parameter specific logistic function evaluated at these points. The calibration employs a nonlinear Gaussian process regression as an interpolator and extrapolator to infer the intermediate values at arbitrary levels of moneyness for which parameter values may be sought. Hyper parameters in the Gaussian process regression were frozen upfront.

Figure 7 presents the stylized true values, the prices at the initial starting point, and the model calibrated values using a single transition matrix as there is no time dependence.



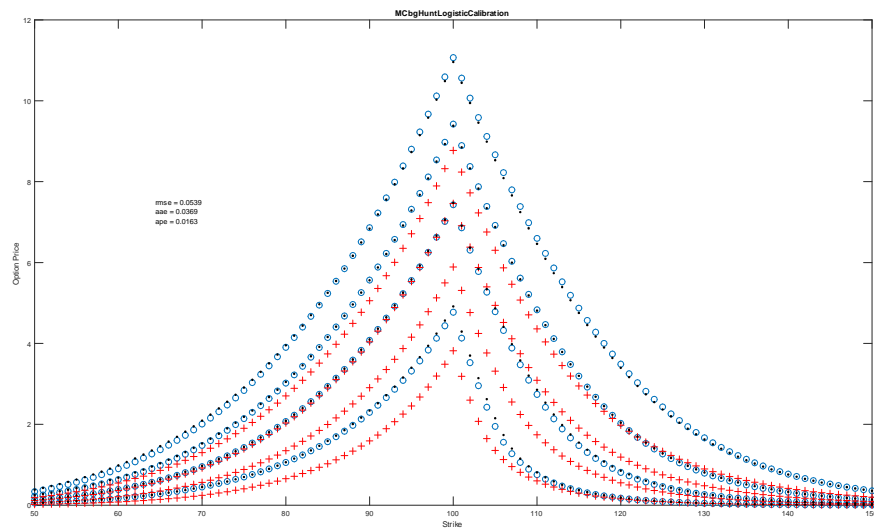


**Figure 7.** Presented by circles are the stylized true values. The plus signs present model prices evaluated at the starting values. The dots are the result of the calibration using an approximating Markov chain with a single transition rate matrix.

The calibrated parameters are presented Table 4.

**Table 4.** Fitted Dependence of Parameters on the level of moneyness.

Grid Level	Calibrated Parameters			
	$b_p$	$c_p$	$b_n$	$c_n$
−0.5	0.0660	0.7066	0.2154	2.0010
−0.2	0.0699	0.7394	0.1871	1.7586
−0.1	0.0692	1.1278	0.1967	2.1669
−0.05	0.0682	1.3565	0.2109	2.0031
0.05	0.0650	2.0245	0.2547	2.1637
0.15	0.0635	2.3484	0.2757	1.9735
0.3	0.0632	2.3750	0.2800	1.5700

Additionally, we present in Figure 8 a graph of the true functional dependence between each of the four parameters and the calibrated dependence as constructed from the values reported in Table 2 using Gaussian process regression with the frozen hyper parameters. We observe that the first four parameters were reasonably well calibrated but the behavior of  $c_n$  was not captured in this exercise.

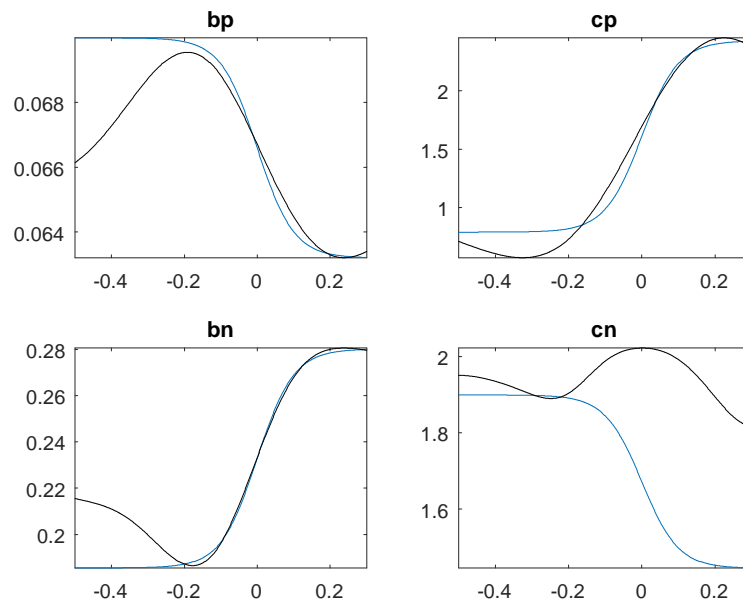
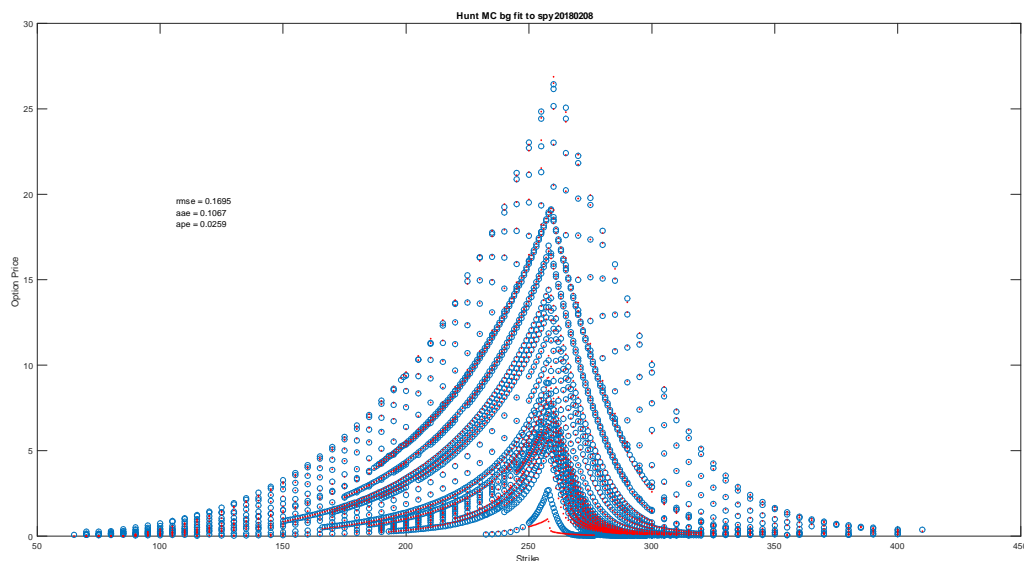


**Figure 8.** The true logistic curve functional dependence is presented in blue. The calibrated dependence as estimated from the implied option prices is presented in black.

### 9. Time and Space Inhomogeneity for Local Bilateral Gamma as Applied to SPY on 8 February 2018

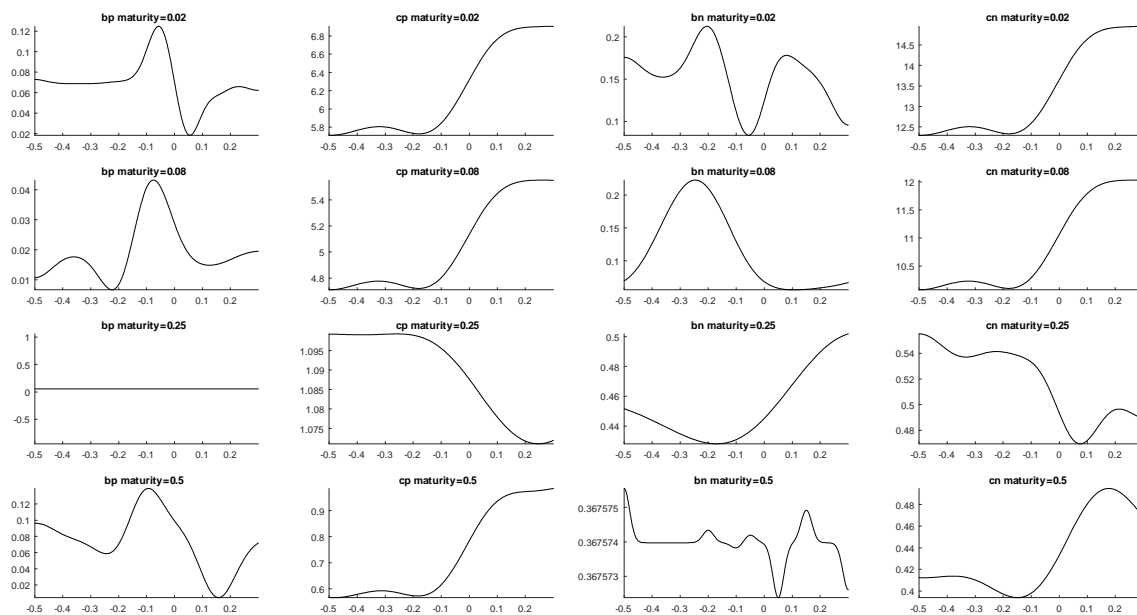
We finally present the results for both a space and time dependence of all four parameters. With a seven point space and time grid each of the four parameters requires a specification of  $49 = 7 \times 7$  values for the space time dependence. The result is a model with  $196 = 49 \times 4$  parameters. As a starting value we used the result from the *bgforward* model for the time dependence. For the space dependence we take the parameter values in the forward model at an intermediate value and a final value and set these as left and right limits for a logistic interpolation using the value  $c = 20$  for the rate at which the logistic function moves from left to right.

Figure 9 presents a graph of the fit along with the fit statistics.



**Figure 9.** Fit of finite state continuous time Markov chain approximation with spatial and temporal inhomogeneity.

Additionally, we present in Figures 10 and 11 the estimated functional dependence of the four parameters on moneyness for the first four and last three maturities respectively.



**Figure 10.** Estimated dependence of the four bilateral gamma parameters on moneyness for the first four maturities.

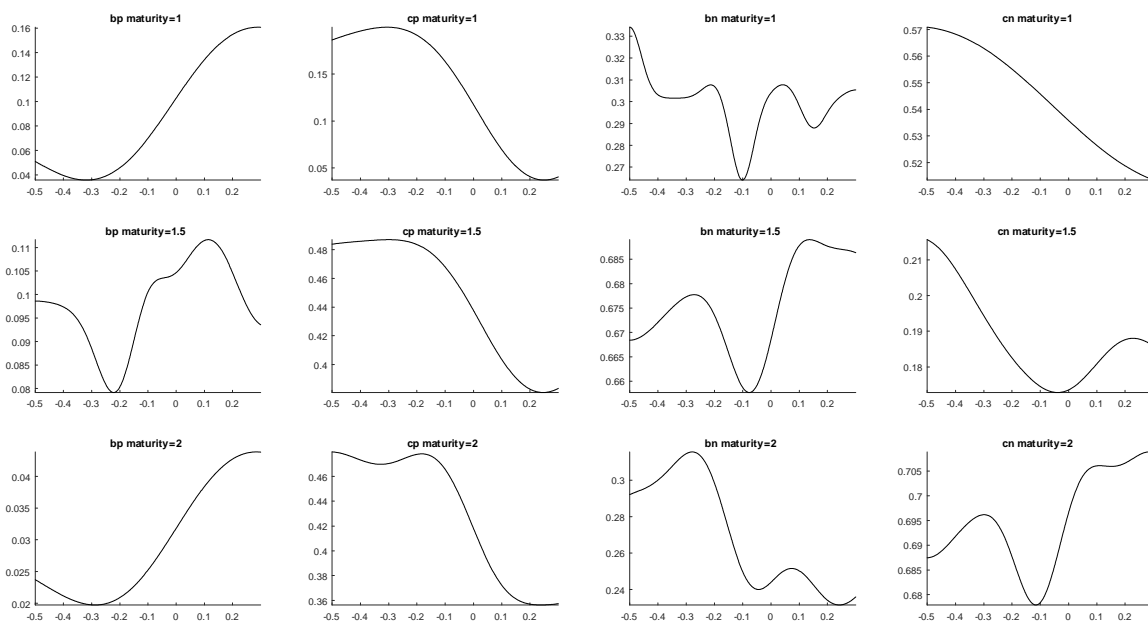


**Figure 11.** Estimated dependence of the four bilateral gamma parameters on moneyness for the last three maturities.

## 10. Conclusions

It is argued that the expansion in the number of maturities being currently quoted and the growth in the associated breadth of strikes involved, renders the use of Fourier inversion methodologies for volatility surface calibration relatively problematic. An alternative of continuous time Markov chain approximation is proposed and shown to be adequate, competitive and it is anticipated that the method is also quite stable. It is at the moment slow to implement but this can be addressed in further research devoted to enhancing its speed.

The Markov chain approximation is also more general and not constrained to working with processes with independent increments. It can accommodate a wide variety of local evolution models though the illustrations of the current paper are restricted to the bilateral gamma process. One may easily incorporate subcases with only time or space inhomogeneity but not both. One may also restrict spatial dependence to a subset of parameters as opposed to allowing them all to change.

Calibrations are illustrated for data on 2695 options across 28 maturities for *SPY* as at 8 February 2018. The Sato process based on the bilateral gamma attains a root mean square error of 0.5140. Just time inhomogeneity with a finite (800) state continuous time Markov chain reduces this to 0.2032. Allowing spatial dependence takes it down further to 0.1695.

**Author Contributions:** Both authors contributed equally to all aspects of this research. Conceptualization, D.B.M. and W.S.; Methodology, D.B.M. and W.S.; Software, D.B.M. and W.S.; Validation, D.B.M. and W.S.; Formal Analysis, D.B.M. and W.S.; Investigation, D.B.M. and W.S.; Resources, D.B.M.; Data Curation, D.B.M. and W.S.; Writing, D.B.M. and W.S.; Visualization, D.B.M. and W.S.

**Funding:** This research received no external funding.

**Conflicts of Interest:** The authors declare no conflict of interest.

## Appendix A

We show that the densities implied by option prices for each maturity are increasing in the convex order. For this we turn to calendar spread arbitrages. Consider two dates  $T < U$  with call options at strikes  $K_T, K_U$ . The longer dated option has a value at the earlier date that exceeds its lower bound, namely the forward contract at the earlier date. The final payoffs satisfy

$$(S_U - K_U)^+ \geq S_U - K_U$$

The value of the longer dated option at the earlier date with known forward dividend yields at rates  $\eta(a)$  and known forward interest rates  $r(a)$  at times  $a$  is  $c(S_T, T; K_U, U)$ , where

$$c(S_T, T; K_U, U) \geq \exp\left(-\int_T^U \eta(a) da\right) S_T - K_U \exp\left(-\int_T^U r(a) da\right).$$

This implies

$$c(S_T, T; K_U, U) \geq \exp\left(-\int_T^U \eta(a) da\right) \left(S_T - K_U \exp\left(-\int_T^U (r(a) - \eta(a)) da\right)\right).$$

The left hand side is also nonnegative and hence

$$c(S_T, T; K_U, U) \geq \exp\left(-\int_T^U \eta(a) da\right) \left(S_T - K_U \exp\left(-\int_T^U (r(a) - \eta(a)) da\right)\right)^+.$$

The initial time zero value of the longer dated option therefore satisfies

$$c(S_0, 0; K_U, U) \geq \exp\left(-\int_0^U \eta(a) da\right) c\left(S_0, 0; K_U \exp\left(-\int_0^U (r(a) - \eta(a)) da\right), T\right)$$

In terms of forward option prices we have

$$\begin{aligned} \exp\left(\int_0^U r(a) da\right) c(S_0; K_U, U) &\geq \exp\left(\int_T^U (r(a) - \eta(a)) da\right) \times \\ &\quad \exp\left(\int_0^T r(a) da\right) c\left(S_0, 0; K_U \exp\left(-\int_T^U (r(a) - \eta(a)) da\right), T\right) \end{aligned}$$

It follows that the forward price of the long dated call struck at  $K_U$  exceeds  $F_U/F_T$  times the forward price of the short dated call struck at  $K_U F_T/F_U$ . Equivalently one may write that

$$\int_0^\infty (S - K)^+ q(S, U) dS \geq \frac{F_U}{F_T} \int_0^\infty \left( S - K \frac{F_T}{F_U} \right)^+ q(S, T) dS. \quad (\text{A1})$$

Consider now a call struck on  $s_U$  with strike  $k$  and forward value

$$\begin{aligned} \int_0^\infty (s - k)^+ \tilde{q}(s, U) ds &= \int_0^\infty \left( \frac{S}{F_U} - k \right)^+ q(S, U) dS \\ &= \frac{1}{F_U} \int_0^\infty (S - k F_U)^+ q(S, U) dS \\ &\geq \frac{1}{F_T} \int_0^\infty (S - k F_T)^+ q(S, T) dS \\ &= \int_0^\infty (s - k)^+ \tilde{q}(s, T) ds \end{aligned}$$

The inequality results on using Equation (A1) with  $K = k F_U$ .

## References

- Ané, Thierry, and Hélyette Geman. 2002. Order Flow, Transaction Clock, and Normality of Asset Returns. *Journal of Finance* 55: 2259–84. [\[CrossRef\]](#)
- Barndorff-Nielsen, Ole Eiler. 1998. Processes of Normal Inverse Gaussian Type. *Finance and Stochastics* 2: 41–68. [\[CrossRef\]](#)
- Black, Fisher, and Myron Scholes. 1973. The Pricing of Options and Corporate Liabilities. *Journal of Political Economy* 81: 637–54. [\[CrossRef\]](#)
- Breedon, Douglas, and Robert H. Litzenberger. 1978. Pricing of State-Contingent Claims Implicit in Option Prices. *Journal of Business* 51: 621–51. [\[CrossRef\]](#)
- Carr, Peter, and Dilip Balkrishna Madan. 1999. Option Valuation Using the Fast Fourier Transform. *Journal of Computational Finance* 2: 61–73. [\[CrossRef\]](#)
- Carr, Peter, and Dilip Balkrishna Madan. 2005. A Note on Sufficient Conditions for No Arbitrage. *Finance Research Letters* 2: 125–30. [\[CrossRef\]](#)
- Carr, Peter, and Dilip Balkrishna Madan. 2009. Saddle Point Methods for Option Pricing. *Journal of Computational Finance* 13: 49. [\[CrossRef\]](#)
- Carr, Peter, and Sergey Nadtochiy. 2017. Local Variance Gamma and Explicit Calibration to Option Prices. *Mathematical Finance* 27: 151–93. [\[CrossRef\]](#)
- Carr, Peter, and Liuren Wu. 2003. The Finite Moment Log-Stable Process and Option Pricing. *Journal of Finance* 58: 753–78. [\[CrossRef\]](#)
- Carr, Peter, Helyette Geman, Dilip Balkrishna Madan, and Marc Yor. 2002. The Fine Structure of Asset Returns: An Empirical Investigation. *Journal of Business* 75: 305–32. [\[CrossRef\]](#)
- Carr, Peter, Helyette Geman, Dilip Balkrishna Madan, and Marc Yor. 2003. Stochastic Volatility for Lévy Processes. *Mathematical Finance* 13: 345–82. [\[CrossRef\]](#)
- Carr, Peter, Helyette Geman, Dilip Balkrishna Madan, and Marc Yor. 2007. Self-Decomposability and Option Pricing. *Mathematical Finance* 17: 31–57. [\[CrossRef\]](#)
- Clark, Peter. K. 1973. A Subordinated Stochastic Process Model with Finite Variance for Speculative Prices. *Econometrica* 41: 135–55. [\[CrossRef\]](#)
- Cui, Zhenyu, Justin Lars Kirkby, and Duy Nguyen. 2017. A general framework for discretely sampled realized variance derivatives in stochastic volatility models with jumps. *European Journal of Operational Research* 262: 381–400. [\[CrossRef\]](#)
- Cui, Zhenyu, Justin Lars Kirkby, and Duy Nguyen. 2018. A general valuation framework for SABR and stochastic local volatility models. *SIAM Journal of Financial Mathematics* 9: 520–63. [\[CrossRef\]](#)
- Davis, Mark, and David Hobson. 2007. The Range of Traded Options. *Mathematical Finance* 17: 1–14. [\[CrossRef\]](#)

- Duffie, Darrell, Jun Pan, and Ken Singleton. 2000. Transform Analysis and Asset Pricing for Affine Jump-Diffusions. *Econometrica* 68: 1343–76. [\[CrossRef\]](#)
- Duffie, Darrell, Damir Filipović, and Walter Schachermayer. 2003. Affine Processes and Applications in Finance. *Annals of Probability* 13: 984–1053.
- Dupire, Bruno. 1994. Pricing with a smile. *Risk* 7: 18–20.
- Eberlein, Ernst, and Ulrich Keller. 1995. Hyperbolic Distributions in Finance. *Bernoulli* 1: 281–99. [\[CrossRef\]](#)
- Eberlein, Ernst, and Karsten Prause. 2002. The generalized hyperbolic model: Financial derivatives and risk measures. In *Mathematical Finance-Bachelier Finance Congress 2000*. Edited by Helyette Geman, Dilip Madan, Stanley Pliska and Ton Vorst. Berlin and Heidelberg: Springer.
- Elliott, Robert James, and Carlton-James U. Osakwe. 2006. Option Pricing for Pure Jump processes with Markov Switching Compensators. *Finance and Stochastics* 10: 250–75. [\[CrossRef\]](#)
- Fang, Fang, and Cornelis W. Oosterlee. 2008. A novel pricing method for European options based on Fourier cosine series expansions. *SIAM Journal of Scientific Computation* 31: 826–48. [\[CrossRef\]](#)
- Fengler, Matthias. 2009. Arbitrage-Free Smoothing of the Implied Volatility Surface. *Quantitative Finance* 9: 417–28. [\[CrossRef\]](#)
- Gatheral, Jim. 2006. *The Volatility Surface: A Practitioner's Guide*. Hoboken: John Wiley.
- Gatheral, Jim, and Antoine Jacquier. 2014. Arbitrage-Free SVI Volatility Surfaces. *Quantitative Finance* 14: 59–71. [\[CrossRef\]](#)
- Guo, Gaoyue, Antoine Jacquier, Claude Martin, and Leo Neufcourt. 2016. Generalized Arbitrage-Free SVI Volatility Surfaces. *SIAM Journal of Financial Mathematics* 7: 619–41. [\[CrossRef\]](#)
- Heston, Steve. 1993. A Closed-Form Solution for Options with Stochastic Volatility with Applications to Bond and Currency Options. *Review of Financial Studies* 6: 327–43. [\[CrossRef\]](#)
- Kirkby, Justin Lars. 2015. Efficient option pricing by frame duality with the fast Fourier transform. *SIAM Journal of Financial Mathematics* 6: 713–47. [\[CrossRef\]](#)
- Kirkby, Justin Lars, Duy Nguyen, and Zhenyu Cui. 2017. A unified approach to Bermudan and barrier options under stochastic volatility with jumps. *Journal of Economic Dynamics and Control* 80: 75–100. [\[CrossRef\]](#)
- Kellerer, Hans G. 1972. Markov-Komposition und eine Anwendung auf Martingale. *Mathematische Annalen* 198: 99–122. [\[CrossRef\]](#)
- Khintchine, Aleksandr Yakolevich. 1938. *Limit Laws of Sums of Independent Random Variables*. Moscow: ONTI.
- Konikov, Mikhail, and Dilip Madan. 2002. Stochastic Volatility via Markov Chains. *Review of Derivatives Research* 5: 81–115. [\[CrossRef\]](#)
- Kou, Steve. 2002. A Jump-Diffusion Model for Option Pricing. *Management Science* 48: 1088–101. [\[CrossRef\]](#)
- Küchler, Uwe, and Stefan Tappe. 2008. Bilateral Gamma Distributions and Processes in Financial Mathematics. *Stochastic Processes and their Applications* 118: 261–83. [\[CrossRef\]](#)
- Lévy, Paul. 1937. *Théorie de l'Addition des Variables Aléatoires*. Paris: Gauthier-Villars.
- Li, Lengfei, and Gongqiu Zhang. 2017. Analysis of Markov chain approximation for option pricing and hedging: Grid design and convergence behavior. *Operations Research*. [\[CrossRef\]](#)
- Madan, Dilip, and Eugene Seneta. 1990. The variance gamma (VG) model for share market returns. *Journal of Business* 63: 511–24. [\[CrossRef\]](#)
- Madan, Dilip, and King Wang. 2017. Asymmetries in Financial Returns. *International Journal of Financial Engineering* 4: 1750045. [\[CrossRef\]](#)
- Madan, Dilip, Carr Peter, and Chang Eric. 1998. The variance gamma process and option pricing. *European Finance Review* 2: 79–105. [\[CrossRef\]](#)
- Madan, Dilip, Wim Schoutens, and King Wang. 2018. Bilateral Multiple Gamma Returns: Their Risks and Rewards. SSRN. [\[CrossRef\]](#)
- Madan, Dilip, Wim Schoutens, and King Wang. 2017. Measuring and Monitoring the Efficiency of Markets. *International Journal of Theoretical and Applied Finance* 20: 1–32. [\[CrossRef\]](#)
- Merton, Robert Cox. 1973. Theory of Rational Option Pricing. *Bell Journal of Economics and Management Science* 4: 141–83. [\[CrossRef\]](#)
- Merton, Robert Cox. 1976. Option Pricing when Underlying Stock Returns are Discontinuous. *Journal of Financial Economics* 3: 125–44. [\[CrossRef\]](#)
- Mijatović, Alexander, and Martijn Pistorius. 2011. Continuously Monitored Barrier Options Under Markov Processes. *Mathematical Finance* 23: 1–38. [\[CrossRef\]](#)



- Niccolato, Elisa, and Emmanouil Vernados. 2003. Option Pricing in Stochastic Volatility Models of the Ornstein-Uhlenbeck type with a Leverage Effect. *Mathematical Finance* 13: 445–66. [\[CrossRef\]](#)
- Rogers, Leonard Christopher Gordan, and O. Zane. 1999. Saddlepoint approximations to option prices. *Annals of Applied Probability* 9: 493–503. [\[CrossRef\]](#)
- Ross, Stephen A. 1978. A Simple Approach to the Valuation of Risky Streams. *Journal of Business* 51: 453–75. [\[CrossRef\]](#)
- Sato, Ken-Iti. 1991. Self similar processes with independent increments. *Probability Theory and Related Fields* 89: 285–300. [\[CrossRef\]](#)
- Xiong, Jian, Augustine Wong, and Donna Salopek. 2005. Saddlepoint approximations to option price in a general equilibrium model. *Statistics and Probability Letters* 71: 361–69. [\[CrossRef\]](#)



© 2019 by the authors. Licensee MDPI, Basel, Switzerland. This article is an open access article distributed under the terms and conditions of the Creative Commons Attribution (CC BY) license (<http://creativecommons.org/licenses/by/4.0/>).